Arab J Sci Eng (2011) 36:1381–1392
DOI 10.1007/s13369-011-0125-x

RESEARCH ARTICLE - MECHANICAL ENGINEERING

Hossein Salari-Rad · Morteza Rahimi-Dizadji · Shiva Rahimi-Pour · Mahmood Delforouzi

Meshless EFG Simulation of Linear Elastic Fracture Propagation Under Various Loadings

Received: 9 December 2009 / Accepted: 23 June 2010 / Published online: 19 October 2011

Abstract We used computational mechanics consisting of various numerical methods to analyze different problems under various boundary conditions. The main advantage of the element free Galerkin (EFG) method is that the model meshing stage is not required and the nodal points are distributed throughout the model domain instead of being meshed. Nodal points are distributed within the model domain to capture a stress singularity around the crack tip. In this paper, various 2D problems in the field of linear elastic fracture mechanics were analyzed to validate the accuracy of the EFG code that was developed in a Matlab environment. To simulate the fracturing process based on the maximum hoop stress criterion, stress intensity factors and the angle of crack propagation were calculated under different loading conditions and the crack trajectory was determined. The obtained results of the developed EFG-code were compared with available experimental data and other numerical (boundary element method and finite element method) methods.

Keywords Element free Galerkin method (EFGM) · Linear elastic fracture mechanics (LEFM) · Stress intensity factor (SIF) · Crack propagation direction · Matlab programming environment

H. Salari-Rad (✉) · M. Rahimi-Dizadji · M. Delforouzi
Department of Rock Mechanics, Faculty of Mining and Metallurgical Engineering,
Amirkabir University of Technology (Tehran Polytechnic), 424 Hafez Ave.,
PO Box 15875-4413, Tehran, Iran
E-mail: salarih@aut.ac.ir

M. Rahimi-Dizadji
E-mail: m.rahimi@aut.ac.ir

M. Delforouzi
E-mail: delforouzi@gmail.com

S. Rahimi-Pour
Faculty of Mathematics and Computer Sciences, Amirkabir University of Technology (Tehran Polytechnic),
424 Hafez Ave., PO Box 15875-4413, Tehran, Iran
E-mail: rahimipour@aut.ac.ir

الخلاصة

تستخدم ميكانيكا الحسابات العددية بطرقها العددية المختلفة لتحليل مشاكل مختلفة لأنواع مختلفة من الشروط الحدية. أساسا إن الميزة الرئيسية لطريقة العنصر الحر لجالركيت (EFG) هي لحذف مرحلة أنموذج الشبكة ولتوزيع نقاط العقد خلال نطاق الأنموذج بدلا عند رسم الشبكة.

وقد تم توزيع النقاط العقدية في النطاق وذلك لالتقاط الإجهاد المصغر حول رأس الشق. هناك مشاكل مختلفة ثنائية الأبعاد 2D في مجال ميكانيكا الكسر المرن الخطي ثم تحليها للتحقق من دقة الشفرة EFGالمطور في بيئة Matlab.

ومن أجل محاكاة عملية الكسر، استنادا إلى أقصى معيار إجهاد داخلي ولمعامل شدة الإجهاد وزاوية انتشار الشقوق فقد تم احتسابها في ظل ظروف التحميل المختلفة ومسار الشقوق. ثم مقارنة النتائج التي تم الحصول عليها للشفرة EFG ومتطلبات الأبحاث التجريبية المتوفرة والعددية (طريقة الشروط الحدية للعنصر وطريقة العنصر المحدود).

List of symbols

$(\sigma_{\theta\max})$	Maximum hoop stress
$(G_{\max})$	Maximum energy release rate
$(S_{\theta\max})$	Strain energy density factor
K_I, K_{II}	Stress intensity factors for mode-I and mode-II
θ_C, θ_0	Angle of crack propagation
β	Angle of crack inclination
a	Half crack length
w_I	Weight function of node I
d_I	Support size of node I
x_I	Coordinate vector of node I
n_i, n_j	Number of nodes are i, j directions
r	Normalized radius
Ω	Domain of problem geometry
Γ	Global boundary
Γ_u	Displacement boundary condition
Γ_t	Traction boundary condition
$\mathbf{u}$	Displacement vector
$\bar{\mathbf{u}}$	Prescribed boundary displacement
$\mathbf{b}$	Vector of body forces
$\bar{t}$	Prescribed boundary tractions
λ	Lagrangian multiplier
$\mathbf{\Phi^T}$	Shape functions matrix
$\mathbf{B}$	Strain–displacement relationship matrix
$\mathbf{N}$	Lagrange interpolation matrix
$\mathbf{D}$	Stress–strain relationship matrix
$\mathbf{f}$	Force vector
$\mathbf{K}$	Stiffness matrix
$\mathbf{G}$	Transition matrix
E	Young's modulus
ν	Poisson's ratio
$\sigma_{T\infty}$	Stress applied in infinite
L	Model length
D	Model width
t	Model thickness

1 Introduction

In linear elastic fracture mechanics crack propagation is modeled by calculating stress intensity factors and the crack initiation direction obtained after doing a stress analysis on the model domain [1]. Computational methods have been used to solve these problems in the engineering field. Many new approaches in computational mechanics such as the finite element method (FEM) [2] and the boundary element method (BEM) [3] have

been used for the analysis of fracture mechanics problems in the wider field of numerical fracture mechanics [4–6]. Although the FEM is a robust and well established technique for the modeling of complicated problems it has some deficiencies because of the mesh-base structure of the FEM. The reliance of the FEM on mesh size and shape leads to complications such as fracture propagation problems in some cases. Subsequently, for the modeling of large deformation fracture propagation and fragmentation processes the accuracy of this method decreases significantly because of the high compression or torsion of the elements. An analysis of these problems by mesh-base methods may require domain remeshing for each step of the progression. On the other hand, continuous remeshing causes a reduction in accuracy and it requires a difficult procedure for code implementation while mesh generation is time-consuming [7,8].

To solve the problem of discretization interfering with the arbitrary crack extension, meshing needs to be removed from the simulation process [9]. Using meshless methods the crack can propagate through a system of nodes, which is enhanced by taking the displacement field into account near the crack tip to precisely capture the stress singularity. Belytschko et al. [8] introduced the element free Galerkin method (EFGM) as a meshless or mesh-free approach and it has applications in computational fracture mechanics [10,11]. The relationships among the meshless category methods have been described previously [7,12].

In the element free Galerkin method (EFGM) a moving least squares (MLS) [13] approximation is used and a linear combination of basis functions fits to data by a weighted function. The MLS approximation is constructed entirely in terms of a set of interior nodes and a description of the model boundaries. The values of desired functions like displacements at any point are obtained by solving a set of linear equations. The size of the system is determined by the number of nodes, which influences the approximation at a point [9]. By analyzing a domain containing a crack the node organization near a fracture tip has an intense impact on the exactness of the stress intensity factor calculation [8].

Alshoaibi and Ariffin [4] calculated stress intensity factors with the FEM by triangular mesh generation using the advancing front method for an elastic-plastic crack growth problem under plane strain and plane stress conditions. In their method, the values of the stress intensity factors (SIFs) in pure mode-I were based on the displacement extrapolation method using the maximum hoop stress criterion.

In this paper, after a brief present of EFGM theory, various 2D problems in the linear elastic fracture mechanics (LEFM) field are modeled using EFG code developed in Matlab. To simulate the fracturing process, the SIFs and the crack initiation angle were calculated under different loading conditions and the crack trajectory was determined using the maximum circumferential stress method. The results obtained from the developed EFG-code were compared with other numerical methods (the FEM and the BEM) and with other experimental research. To carry out a meaningful comparison the input parameters of the EFG code were selected based on available experimental and numerical data (BEM and FEM) from other reported work.

2 Mechanics of Linear Elastic Fracture Propagation

The classic general objective of fracture mechanics is to determine the rate of change for an existing crack [9]. Crack propagation is determined by the stress and strain fields of the crack tip in its instantaneous vicinity. To determine the behavior of cracked domains and to correlate this with experimental data, crack tip fields must be inferred. In the LEFM the SIFs are significant parameters that can be applied to various loading conditions, which leads to different failure modes.

Several methods have been proposed to determine SIFs such as the energy domain integral method [14], the J-integral method [15,16] and displacement extrapolation near the crack tip [17,18]. In this paper, the path-independent J-integral method was used to calculate SIFs based on the ratio of the relative crack tip displacement determined using the EFGM. Basic definitions and a complete procedure for the accurate determination of the J-integral have been reported previously [15,16]. For the simulation of fracture propagation using the LEFM the fracture trajectory direction must be determined. Many criteria to evaluate fracture propagation direction have been reported in the literature and these are critical dilatational strain energy (T-criterion) [19], the maximum stress triaxiality criterion (M-criterion) [20], the minimum radius criterion (R-criterion) [21], the maximum hoop stress ($\sigma_{\theta\max}$) criterion [22], the maximum energy release rate ($G_{\max}$) criterion [23] and the strain energy density factor ($S_{\theta\max}$) criterion [24]. We used maximum hoop stress theory wherein the crack tip is extended in the direction where the circumferential stress is at a maximum and the direction of crack propagation θ_C is determined as follows:

$$K_I \sin\theta_C + K_{II}\,(3\cos\theta_C - 1) = 0 \tag{1}$$

Khan and Khraisheh [21] carried out a comprehensive comparison between the above-mentioned criteria. Despite the fact that these criteria represent various viewpoints all these methods produce comparable results and empirically recognizable differences have not been reported [25]. Based on Eq. (1) the crack propagation direction is $\theta_C = 0$ for pure mode-I ($K_{II} = 0$) and the propagation angle is $\theta_C = \pm 70.5$ for pure Mode-II ($K_I = 0$).

$$\theta_C = 2 \arctan \left(\frac{1}{4} \frac{K_I}{K_{II}} \pm \frac{1}{4} \sqrt{\left(\frac{K_I}{K_{II}} \right)^2 + 8} \right) \tag{2}$$

3 Overview of the EFGM

The main objective of meshless methods is to remove or diminish the difficulty of meshing and remeshing the entire structure by only adding or deleting nodes within the entire structure. Each node is associated with a domain of influence and supports a weight function $w_I(x)$ with $w_I(x) > 0$ within the domain of influence and $w_I(x) = 0$ outside the domain of influence [7,11]. Figure 1 shows that the domains of influence for nodes are typically circular or rectangular areas.

Weight functions $w_I(\mathbf{x}_I)$ play a significant role in meshless methods. They should be constructed positively so that a unique solution of shape functions is assured. Additionally, they should be relatively large for x_I near x and comparatively small for more distant x_I [12,26]. The cubic spline weight function is applied in this paper as suggested in previous work [27] and it is shown as a function of r in Fig. 2.

$$w(r) = \begin{cases} \frac{2}{3} - 4r^2 + 4r^3 & r \leq 1 \\ \frac{4}{3} - 4r + 4r^2 - \frac{4}{3}r^3 & \frac{1}{2} < r \leq \frac{1}{2} \\ 0 & r > 1 \end{cases} \tag{3}$$

with

$$r = \frac{\|x_I - x\|}{d_I}$$

where d_I is the support size of the node.

The discretization of the governing equations by the EFG method requires a least square approximation composed of three constituents that contain a weight function related to each node, a set of non-constant coefficients and a monomial basis function. A complete formulation of the MLS was given in previous work [13].

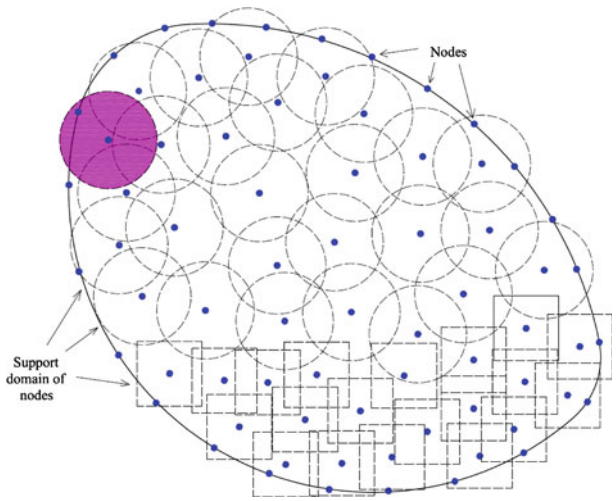

Fig. 1 Model discretization using a meshless method

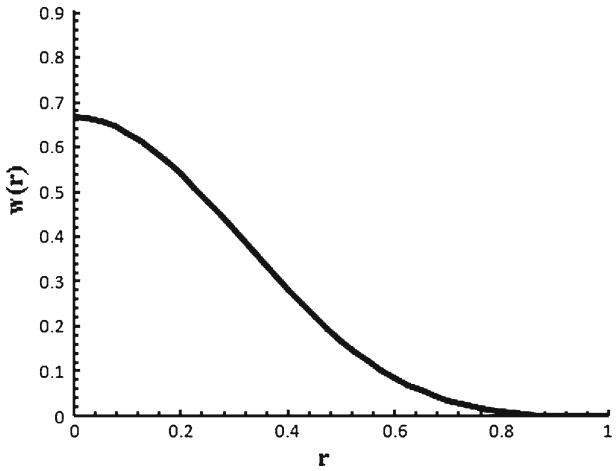

Fig. 2 Cubic spline weight function over the normalized distance r

3.1 Discrete Equations and Integration

For a two-dimensional problem on the domain Ω bounded by Γ in elasticity mechanics, u is the displacement field on Ω, b is the body force, $\bar{u}$ is the boundary values of the displacement boundary, and Γ_u and $\bar{t}$ are the boundary values on the traction boundary Γ_t. In the EFGM the final discrete equation for this case is [10]:

$$\begin{bmatrix} \mathbf{K} & \mathbf{G} \\ \mathbf{G^T} & \mathbf{0} \end{bmatrix} \begin{Bmatrix} \mathbf{u} \\ \lambda \end{Bmatrix} = \begin{Bmatrix} \mathbf{f} \\ \mathbf{q} \end{Bmatrix} \tag{4}$$

where

$$\mathbf{f} = \int_{\Omega} \mathbf{\Phi^T} \mathbf{b} \mathrm{d}\Omega + \int_{\Gamma_t} \mathbf{\Phi^T} \bar{\mathbf{t}} \mathrm{d}\Gamma \tag{5}$$

$$\mathbf{q} = -\int_{\Omega} \mathbf{N^T} \bar{\mathbf{u}} \mathrm{d}\Gamma \tag{6}$$

$$\mathbf{K} = \int_{\Omega} \mathbf{B^T D B} \mathrm{d}\Omega \tag{7}$$

$$\mathbf{G} = -\int_{\Omega} \mathbf{\Phi^T N} \mathrm{d}\Gamma \tag{8}$$

In the above equations, λ is the Lagrange multipliers that were applied to satisfy the essential boundary conditions because the shape functions for the MLS approximation do not meet the essential boundary conditions exactly, $\mathbf{\Phi^T}$ is the shape functions matrix for the MLS approximation [28], **B** is the strain–displacement relationship matrix for the MLS approximation [13], **N** is the Lagrange interpolation matrix and **D** is the stress–strain relationship matrix, which is defined as follows:

$$D = \begin{cases} \dfrac{E}{(1-v^2)} \begin{bmatrix} 1 & v & 0 \\ v & 1 & 0 \\ 0 & 0 & \dfrac{(1-v)}{2} \end{bmatrix} & \text{plane stress} \\ \dfrac{E}{(1+v)(1-2v)} \begin{bmatrix} 1-v & v & 0 \\ v & 1-v & 0 \\ 0 & 0 & \dfrac{(1-2v)}{2} \end{bmatrix} & \text{plane strain} \end{cases} \tag{9}$$

here, E and v are Young's modulus and Poisson's ratio, respectively.

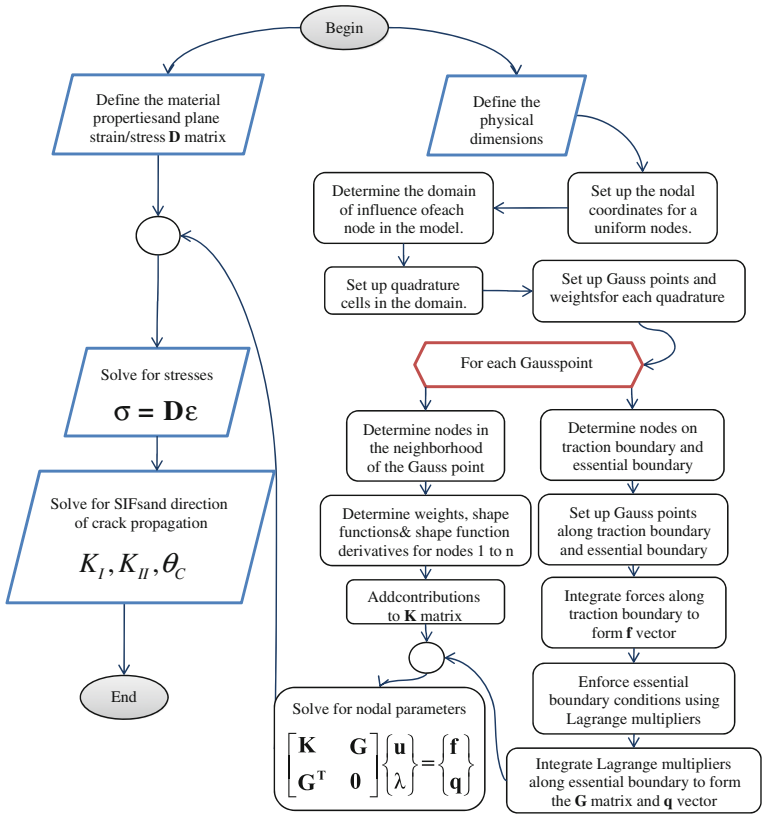

Fig. 3 Flowchart for the extraction of SIFs and the crack initiation angle in the EFG code

To integrate the stiffness matrix (Eq. 7) and the force vector (Eq. 5), a Guassian quadrature is used for the interior of the solution domain and its boundary. In general, a 4×4 quadrature is adequate but for more precise results, particularly in the cells that surround the fracture tip, a 8×8 quadrature may be used for integration [29]. However, rezoning effects are very small and they do not seem to guarantee any consequent intricacies.

3.2 General Coding Procedure

The general EFG coding algorithm for 2D problems as proposed by Dolbow and Belytschko [27] can be depicted in Fig. 3:

The algorithm was coded in the MATLAB programming environment because of its good matrix manipulation performance. In the first step of the program, the model geometry ($L \times D$) is defined and the nodal coordinates ($\mathbf{x}$) are set up while the nodes ($n_i \times n_j$) are distributed uniformly within the model domain. In the second step the parameters of the weight function ($w_I(\mathbf{x} - \mathbf{x_I})$) and the node's domain of influence (d_I) are set. In the third step integration points and weights are determined. To assemble the discrete equations, a loop over is required for each integration point to determine all the matrices. After solving the system of obtained equations the displacement field is determined within the model domain ($\mathbf{u}$). By multiplying the stiffness of the model material ($\mathbf{D}$) with the strain ($\boldsymbol{\varepsilon}$) the stress field is obtained. Based on the obtained stresses, SIFs (K_I, K_{II}) are calculated and finally the new crack propagation direction (θ_C) is calculated.

4 Numerical Simulation

To carry out an extensive evaluation of the SIFs and the fracture propagation direction the EFG developed code was used to evaluate the SIFs and the crack initiation angle for the LEFM under plane strain and plane stress conditions.

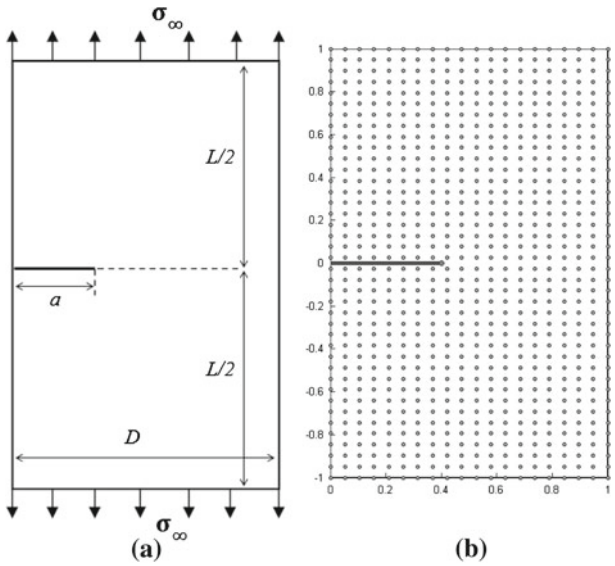

Fig. 4 **a** Problem statement and **b** nodal distribution before fracture propagation for the *edged horizontal crack*

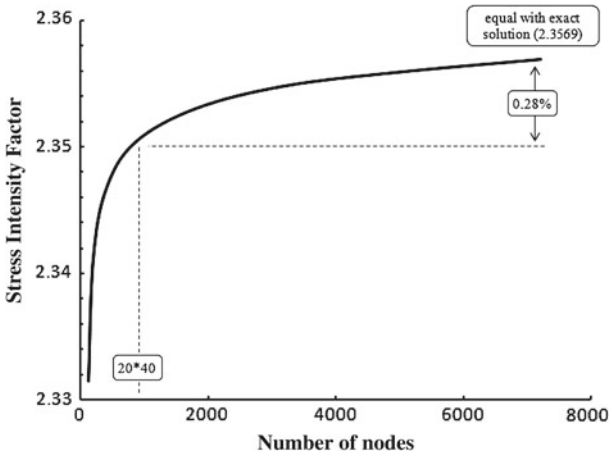

Fig. 5 Sensitivity analysis of the number of nodes in the SIF calculation

4.1 Rectangular Plate with a Single Edge Crack Under Tension

The model geometry and its discretized meshless model for a single edge cracked rectangular plate under plane stress are shown in Fig. 4. The model crack situation is shown in the first step before fracture propagation.

The plate has an initial crack length of $a = 0.4$ units, a plate length of $L = 2$ units, a plate width of $D = 1$ units and a thickness of $t = 1$ unit while the 800(20×40) uniform nodes are constructed for an MLS approximation. To choose a nodal density for each analysis a sensitivity analysis was carried out and the obtained values were compared. As for FE analysis the mesh density varies in different cases when trying to determine the optimum conditions for meshing. Fig. 5 shows a comparison of the various nodal densities for this problem and the calculated SIF values. As shown in Fig. 5, when the number of nodes is larger than 800 (20×40) the SIF value does not change considerably and the maximum error is about 0.28%.

The tensile stress for the upper and lower bounds of the model was $\sigma_{T\infty} = 1$. The other input parameters are presented in Table 1.

Table 1 Input parameters for the meshless model

Model configuration	Plane stress
Model dimensions	$L \times D = 2 \times 1$
Crack length	$a = 0.4$
Stress applied in infinite	$\sigma_{T\infty} = 1$
Elastic modulus	$E = 1 \times 10^6$
Poisson's ratio	$\upsilon = 0.3$
Nodal distribution	$n = 40 \times 80$
Domain of support	Circular

Table 2 Values of the calculated SIFs determined by different methods

Method	Calculated stress intensity factor
Exact solution [31]	2.3570
FEM [4]	2.3415
Hybrid [30]	2.3441
EFG code (present study)	2.3503

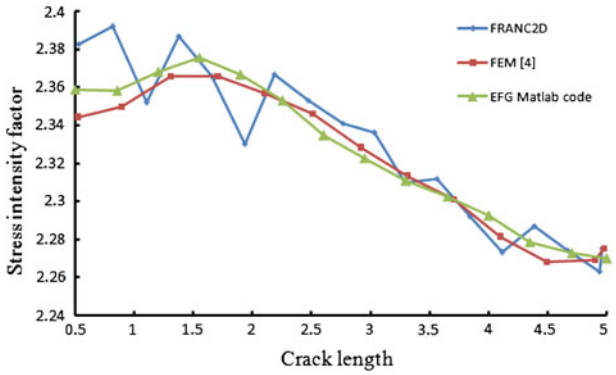

Fig. 6 Similarity of the calculated SIFs from FEM [4] results, the FRANC2D program and EFG code (this study)

Alshoaibi and Ariffin [4] evaluated the value $K_I = 2.3415$ using FEM with an adaptive posteriori h-type mesh refiner using a norm stress error estimator and the maximum hoop stress criterion. Additionally, Rao and Rahman [30] evaluated SIF values for a similar boundary and model geometry using a hybrid FEM/meshless method. The pure mode-I SIF of 2.357 was calculated based on its exact solution in [31] as,

$$K_I = \sqrt{\pi} C \sigma a, \tag{10}$$

where $C = 1.12 - 0.231\left(\frac{a}{D}\right) + 10.55\left(\frac{a}{D}\right)^2 - 21.72\left(\frac{a}{D}\right)^3 + 30.39\left(\frac{a}{D}\right)^4$.

In Table 2 the EFG Matlab code results are compared with the analytical value of the SIF in pure mode-I based on previous work [31] and the results of other methods. It is obvious in Table 2 that using the Matlab developed EFG code the expected SIF values agree well with the exact value of K_I. Additionally, the EFG code output gave a SIF value for 7,200 nodes of $K_I = 2.3569$, which approaches the exact value obtained by the closed-form method in previous work [31].

A further analysis of the fracture propagation steps was carried out by changing the model size to $L \times D = 20 \times 10$ and the initial crack length to $a = 0.5$ and SIFs were obtained using the developed EFG code. These values were compared with those calculated by a program developed by Cornell Fracture Group (FRANC2D/L) as well as FEM results from Alshoaibi and Ariffin [4] with a similar fracture propagation criterion and boundary conditions. Results of these comparisons are shown in Fig. 6 and the agreement is good.

In fact, the fracture propagation trends are almost the same in all cases as shown in Fig. 6. Additionally, the obtained crack propagation behavior based on the EFGM lies between the two other procedures.

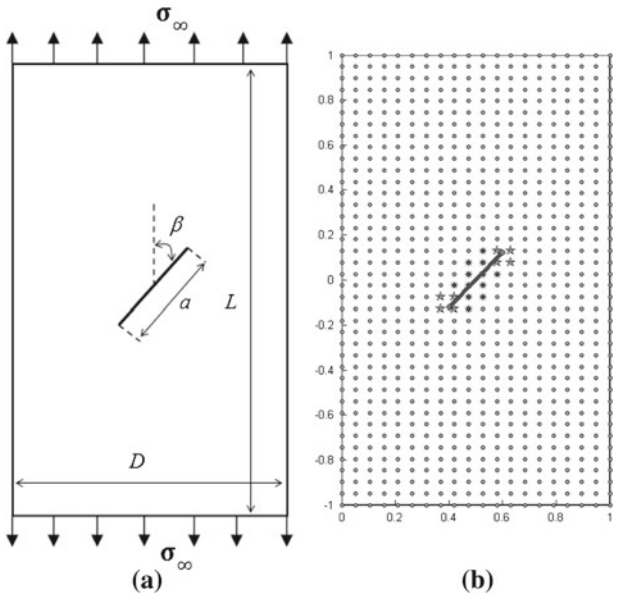

Fig. 7 Problem statement (**a**) and the nodal distribution (**b**) before fracture propagation for a centered slanted crack

Table 3 Input parameters for the meshless model

Model configuration	Plane stress
Model dimensions	$L \times D = 10 \times 10$
Crack length	$a = 0.3$
Stress applied in infinite	$\sigma_{T\infty} = 1$
Elastic modulus	$E = 1 \times 10^7$
Poisson's ratio	$\upsilon = 0.3$
Nodal distribution	$n = 40 \times 40$
Crack dip	$\beta = 40°$

4.2 Rectangular Plate with a Centered Slant Crack

A rectangular plate containing a slanted crack was subjected to uniaxial tension in a plane strain problem as depicted in Fig. 7.

The geometry of the domain and the model discretization is the same as that used for the single edge cracked plate shown in Fig. 7 and Table 3. Uniaxial tension was applied along the vertical direction, as shown in the figure. This leads to the asymmetric Mode-II loading condition.

The calculated values for K_I and K_{II} in mixed mode growth for the 5 step fracture propagation process are depicted in Fig. 8b. K_I increases with step extension and K_{II} decreases with crack growth. The crack propagation direction, θ_0, based on the values of K_I and K_{II} and the selected crack growth criterion were calculated and the final crack trajectory is depicted in Fig. 8a. The crack grows in the direction that finally tends to be perpendicular to the maximum hoop stress.

Erdogan and Sih [22] performed uniaxial tension tests on isotropic Plexiglass sheets ($229 \times 457 \times 4.8$ mm) containing a 50.8 mm central crack. To predict the crack propagation these tests were simulated using the developed EFG code. Chen et al. [6] reproduced these tests using another numerical method (BEM) with the same domain geometry and boundary conditions. The angle of fracture initiation using different crack orientation angles was calculated to validate the developed EFG code.

The results obtained from the developed EFG code were compared with those calculated using the BEM by Chen et al. [6] and with experimental results [22] using the same boundary and loading conditions for the plane stress condition based on the maximum hoop stress criterion. The results of this comparison are shown in Fig. 9. This figure shows that the calculated values of the initiation angles are closer to the experimental results than the BEM results. For example, in the case of $\beta = 30°$, the BEM [6] has an error of about 5% and the EFG code has an error of about 1% relative to the experimental data [22].

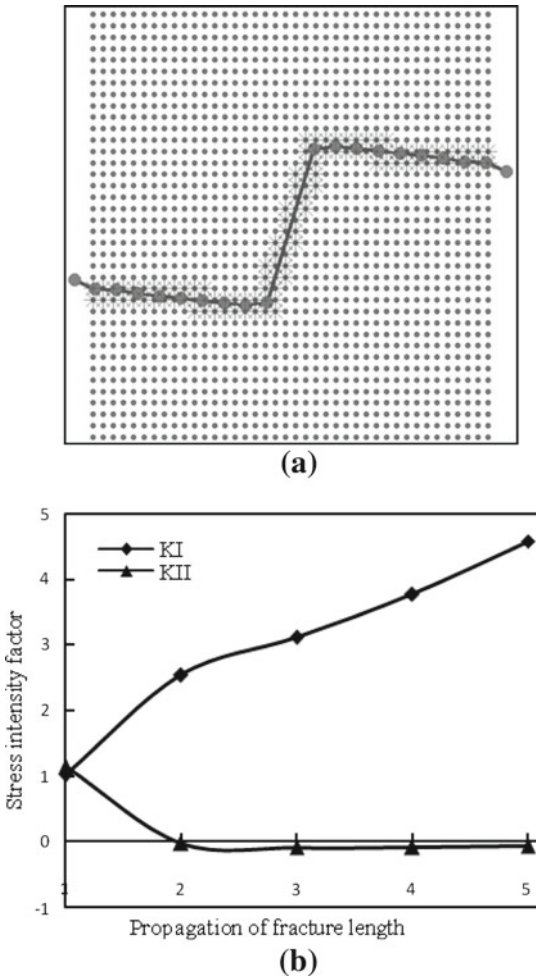

Fig. 8 Output of the meshless model as **a** the final fracture propagation trajectory (Matlab code output) and **b** the calculated SIFs

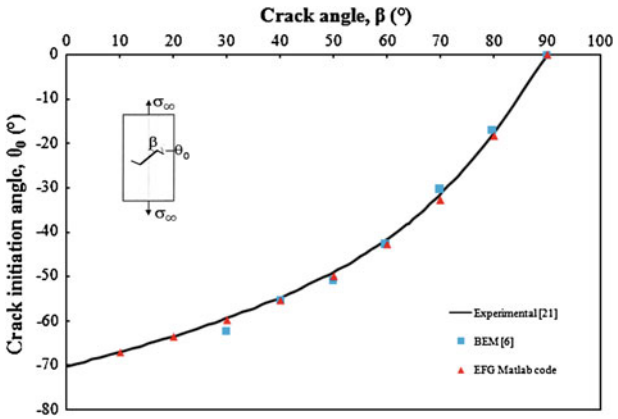

Fig. 9 Variation in the crack initiation angle θ_0 with the crack angle β under uniaxial tension. Experimental results [16], BEM [4] and EFGM (this study)

5 Conclusion

The meshless EFG method shows great promise in engineering applications because of its flexibility in solving problems because of discontinuities in fracture mechanics and large deformations. The aim of this paper was

to evaluate the capability of Matlab developed EFG code in the analysis of crack propagation problems and to compare the accuracy of common numerical methods for the extraction of SIFs and the propagation trajectory of fractures.

Meshless element free Galerkin code using the MLS approximation was developed to simulate fracture propagation based on linear elastic fracture mechanics. Nodal points were scattered within the model domain to capture the stress singularity around the crack tip. The SIFs and the crack initiation angle were predicted using the developed EFG code for a uniaxial loading. The SIFs that were predicted using the EFG code coincide well with those of a standard solution [31] and those from related publications [4,6,30] as well as with a fracture growth program developed by the Cornell Fracture Group (FRANC2D/L). The evaluated crack growth trajectory demonstrated the ability of the developed code to solve fracture propagation problems under various loading conditions.

This code may be extended to the study of anisotropic materials that contain many discontinuities such as faults and joints within a rock or soil mass, which makes it more applicable to practical problems.

Acknowledgments The authors wish to thank to Rock Mechanics Division at Amirkabir University of Technology (Tehran Polytechnic) for providing the facilities to run the numerical models. Also, special thanks to Professor Erdoghan's group for the use of their valuable experimental data.

References

1. Anderson, T.L.: Fracture mechanics, Fundamentals and Applications. Department of Mechanical Engineering, Texas A&M University, Texas, USA (1994)
2. Morozov, E.M.; Nikishkov, G.P.: Use of the finite-element method in fracture mechanics. J. Mater. Sci. **18**(4), 299–314 (1983)
3. Cruse, T.A.: Two-Dimensional BIE fracture mechanics analysis. Appl. Math. Model. **2**, 287–293 (1978)
4. Alshoaibi, M.; Ariffin, A.K.: Finite element simulation of stress intensity factors in elasto-plastic crack growth. J. Zhejiang Univ. Sci. A **7**(8), 1336–1342 (2006)
5. Phongthanapanich, S.; Dechaumphai, P.: Adaptive Delaunay triangulation with object-oriented programming for crack propagation analysis. Finite Element Anal. Des. **40**, 1753–1771 (2004)
6. Chen, Ch. Sh.; Ernian, P.; Amadei, B.: Fracture mechanics analysis of cracked discs of anisotropic rock using the boundary element method. Int. J. Rock Mech. Min. Sci. **35**, 195–218 (1998)
7. Liu, GR.: MeshFree Methods Moving Beyond the Finite Element Methods, 1st edn. CRC Press, Boca Raton, 2003
8. Belytschko, T.; Lu, Y.Y.; Gu, L.: Element-free Galerkin methods, Int. J. Numer. Methods Eng. **37**, 229–256 (1994)
9. Ingraffea, A.R.: Computational Fracture Mechanics, Encyclopedia of Computational Mechanics, vol. 2, issue no. 11. Wiley, New York (2007)
10. Belytschko, T.; Lu, Y.Y.; Gu, L.: Crack propagation by element free Galerkin methods. Eng. Fract. Mech. **51**, 295–315 (1995)
11. Belytschko, T.; Lu, Y.Y.; Gu, L.; Tabbara, M.: Element free Galerkin methods for static and dynamic fracture. Int. J. Solids Struct. **32**, 2547–2570 (1995)
12. Belytschko, T.; Krongauz, Y.; Organ, D.; Fleming, M.; Krysl, P.: Meshless methods: an overview and recent developments. Comput. Methods Appl. Mech. Eng **139**, 3–47 (1996)
13. Liew, K.M.; Feng, C.; Cheng, Y.; Kitipornchai, S.: Complex variable moving least-squares method: a meshless approximation technique. Int. J. Num. Methods Eng. **120**(4), 110–121 (2007)
14. Moran, B.; Shih, C.F.: A general treatment of crack tip contour integrals. Eng. Fract. Mech. **35**, 295–310 (1987)
15. Rice, J.R.: A path independent integral and the approximate analysis of strain concentration by notches and cracks. J. Appl. Mech. **35**, 379–386 (1968)
16. Li, F.Z.; Shih, C.F.; Needleman, A.: A comparison of methods for calculating energy release rates. Eng. Fract. Mech. **21**, 405–421 (1985)
17. Guinea, G.V.; Planas, J.; Elices, M.: KI evaluation by the displacement extrapolation technique. Eng. Fract. Mech. **66**(3), 243–255 (2000)
18. Ma, F.; Deng, X.; Sutton, M.A.; Newman, J.C.: A CTOD-Based Mixed-Mode Fracture Criterion Mixed-Mode Crack Behavior. ASTM STP 1359, pp. 86–110 (1999)
19. Andrianopolous, N.P.; Theocaris, P.S.: LEFM brittle and ductile fractures as described by the T-criterion. Eng. Fract. Mech. **30**(1), 5–12 (1988)
20. Kong, X.M.; Schluter, N.; Dahl, W.: Effect of triaxial stress on mixed-mode fracture. Eng. Fract. Mech. **52**(2), 379–388 (1995)
21. Khan, Sh.M.A.; Khraisheh, M.K.: A new criterion for mixed mode fracture initiation based on the crack tip plastic core region. Int. J. Plast. **20**(1), 55–84 (2004)
22. Erdogan, F.; Sih, G.C.: On the crack extension in plates under plane loading and transverse shear. J. Basic Eng. **85**(B7), 519–527 (1963)
23. Nuismer, R.J.: An energy release rate criterion for mixed mode fracture. Int. J. Fract. **11**(2), 245–250 (1975)
24. Sih, G.C.: Strain–energy–density factor applied to mixed-mode crack problems. Int. J. Fract. **10**(3), 305–321 (1974)
25. Dillard, D.A.; Pocius, A.V.; Chaudhury, M.: Adhesion Science and Engineering, vol. 1. The Mechanics of Adhesion, vol. 11, issue no. 1.2. Elsevier, Amsterdam (2002)

26. Beissel, S.; Belytschko, T.: Nodal Integration of the Element-free Galerkin Method. Comput. Methods Appl. Mech. Eng. **139**, 49–74 (1996)
27. Dolbow, J.; Belytschko, T.: An introduction to programming the meshless element free galerkin method. Arch. Comput. Methods Eng. **5**(3), 207–241 (1998)
28. Mukhrejee, Y.X.; Mukhrejee, S.: On boundary conditions in the element-free Galerkin method. Comput. Mech. **19**(4), 264–270 (1997)
29. Fleming, M.; Chu, Y.A.; Moran, B.; Belytschko, T.; Lu, Y.Y.; Gu, L.: Enriched element-free galerkin methods for crack-tip fields. Int. J. Numer. Methods Eng **40**, 280–314 (1997)
30. Rao, B.N.; Rahman, S.: A coupled meshless-finite element method for fracture analysis of cracks. Int. J. Press. Vessels Piping. **78**(9), 647–657 (2001)
31. Tada, H.; Paris, P.C.; Irwin, G.R.: The Stress Analysis of Cracks Handbook. ASME Press, New York (2000)